

Journal Pre-proofs

Ag nanoparticle immobilized on functionalized magnetic hydrotalcite ($\text{Fe}_3\text{O}_4/\text{HT-SH-Ag}$) for clean oxidation of alcohols with TBHP

Mehri Salimi, Azadeh Zamanpour

PII: S1387-7003(20)30671-7
DOI: <https://doi.org/10.1016/j.inoche.2020.108081>
Reference: INOCHE 108081

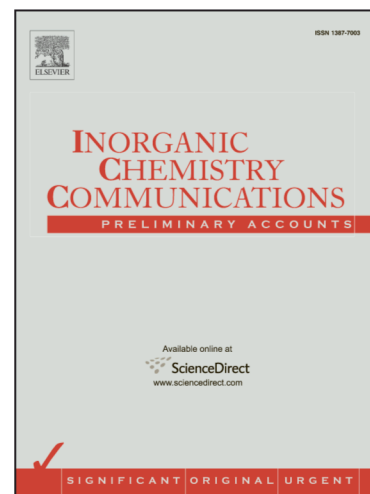
To appear in: *Inorganic Chemistry Communications*

Received Date: 6 June 2020
Revised Date: 23 June 2020
Accepted Date: 28 June 2020

Please cite this article as: M. Salimi, A. Zamanpour, Ag nanoparticle immobilized on functionalized magnetic hydrotalcite ($\text{Fe}_3\text{O}_4/\text{HT-SH-Ag}$) for clean oxidation of alcohols with TBHP, *Inorganic Chemistry Communications* (2020), doi: <https://doi.org/10.1016/j.inoche.2020.108081>

This is a PDF file of an article that has undergone enhancements after acceptance, such as the addition of a cover page and metadata, and formatting for readability, but it is not yet the definitive version of record. This version will undergo additional copyediting, typesetting and review before it is published in its final form, but we are providing this version to give early visibility of the article. Please note that, during the production process, errors may be discovered which could affect the content, and all legal disclaimers that apply to the journal pertain.

© 2020 Elsevier B.V. All rights reserved.



Ag nanoparticle immobilized on functionalized magnetic hydrotalcite (Fe₃O₄/HT-SH-Ag) for clean oxidation of alcohols with TBHP

Mehri Salimi*, Azadeh Zamanpour

Department of Chemistry, Faculty of Science, University of Birjand, P. O. Box 97175-615, Birjand, Iran

*Correspondence to: msalimi@birjand.ac.ir, m_salimi4816@yahoo.com

ORCID: 0000-0003-1755-7297

Abstract:

Hydrotalcite (HT) modified with magnetic nanoparticle and thiol groups for the immobilization of silver to the preparation of Fe₃O₄/HT-SH-Ag was used. The catalyst was completely characterized using XRD, ICP, SEM, EDS, VSM, FT-IR, and TEM analyzes. The Fe₃O₄/HT-SH-Ag catalyst is useful in oxidizing of primary and secondary aliphatic and benzyl alcohols to the relevant carbonyl products (aldehyde/ketone). To demonstrate the effect of Ag over the reaction, Fe₃O₄/HT-SH catalyst performance, and also some other control tests were studied. For this purpose, the model reaction was carried out in the presence of AgNO₃, HT (I), and Fe₃O₄/HT (II), and low yield was obtained (20-50%). High to good efficiency were obtained for all entries, whether benzaldehyde derivatives, in short times. The catalyst can be reused for several continuous runs with a simple external magnet without losing significant reactivity.

Keywords: Oxidation of alcohol, TBHP, hydrotalcite, Fe₃O₄/HT-SH-Ag

1. Introduction

Oxidation reactions catalyzed transition metal complexes are of paramount importance in recent decades [1]. The presence of these active sites are abundant homogeneous transition metal complex catalysts improve their performance, but this complex separation from the reaction mixture is difficult without doubt [2]. Therefore heterogenization via immobilization of transition metal complex onto solid supports to produce a powerful catalyst.

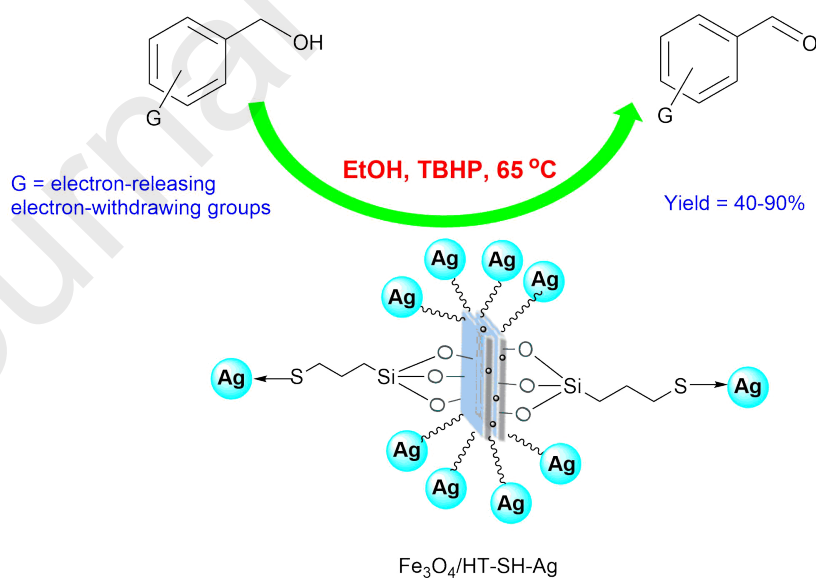
In the last several decades, similar to hydrotalcite compounds (HT) and magnetic hydrotalcite (MHTs) have numerous applications, particularly as catalyst forerunner for the transesterification and as catalysts used for the aldol condensation [3]. The hydrotalcite (HT) has also been proven as efficient support for a wide variety of reactions like oxidation reaction [4], the reduction chemoselective [5], and dehydrogenation [6], because it shows a basic site surface tunable and uniform deposition of the active metal onto the surface

Therefore, the combination of magnetic nanoparticle (MNP) in the structure of hydrotalcite [7] provides simple separation of the catalyst in the reaction medium with the modest magnetic in addition to preventing MNP aggregation, too. To achieve specific goals, metal nanocomposites can be utilized on a large scale. Nanocomposites based on silver have broad applications in various fields like food packaging [8], biosensor [9], and wooden wardrobe [10]. Lately, based on magnetic nanocomposite, silver nanoparticles have been reported as a catalyst and are utilized in the oxidation reaction [11].

Amongst the organic transformation achieved with heterogeneous catalysis, the selective oxidation reaction is widely utilized in synthetic organic chemistry [12–14]. The catalytic oxidation of alcohols has gained considerable attention from an industrial and academic point of view [15]. Carbonyl compounds like ketone and aldehyde derivatives act as important intermediates and precursors in the agrochemical, cosmetics, pharmaceutical, biofuels, insecticides, and confectionery, flame-retardants, and fragrances industries [16]. The oxidation

of alcohol to carbonyls requires not only costly, polluting, and toxic oxidants, for example (hypochlorite chromate, or permanganate, etc.) and difficult reaction circumstances, but also produce significant amounts of pollutants and poisonous waste [17]. Newly, numerous efforts have given to developing more eco-friendly procedures by utilizing cleaner oxidants to minimizing the deficiencies of traditional oxidation methods [18,19]. For environmental concerns and economics, the development of green oxidants has attracted much important consideration.

In continuance of our ongoing project, with the aim of selective oxidation of primary and secondary alcohols and their importance and given all of the reasons mentioned above (mainly the environmentally good character of magnetic hydroxalcite) and silver nanoparticles, it encouraged us to the preparation of $\text{Fe}_3\text{O}_4/\text{HT}/\text{SH}/\text{Ag}$ to produce aldehydes and ketones. To improve the separation of the catalyst, magnetic support was used to immobilize the Ag nanoparticle (Scheme 1).



Scheme 1. Oxidation of alcohols with $\text{Fe}_3\text{O}_4/\text{HT-SH-Ag}$

2. Experimental:

2.1. General

All solvents and chemical reagents were purchased from Sigma-Aldrich and Merck companies and were utilized as received without additional purification. Determinations of purity of the products were performed by thin-layer chromatography on the silica gel plate's polygram STL G/UV 254. The FTIR spectrum was reported on KBr pressed pellet utilizing a spectrometer FTIR Nicolet 800 at room temperature (approximately 400-4000 cm^{-1}). All results related to the product isolated purification afterward with recrystallization or thin-layer chromatography.

2.2. HT synthesis (I)

$\text{Mg}(\text{NO}_3)_2 \cdot 6\text{H}_2\text{O}$ (40 mmol, 10.25 g) and $\text{Al}(\text{NO}_3)_3 \cdot 9\text{H}_2\text{O}$ (20 mmol, 7.5 g) dissolved in water (60 mL) followed by dropwise addition of NaHCO_3 (25 mmol, 2.1 g), and NaOH (100 mmol, 4 g) by heating at 60 °C for 24 hours underwent vigorous magnetic stirring.

After this period, the acquired product (white solid) was separated by filtered and washed with deionized (DI) water (pH=7). The Mg-Al hydrotalcite (I) obtained (molar ratio Mg/Al =2) was dried for 12 hours at 80 °C.

2.3. Fe_3O_4 /HT synthesis

In a 500 mL 3-necked flask, the inert atmosphere was retained via a continuous flow of argon and a dropping funnel, a combination of FeCl_2 (5.2 mmol, 1.05 g) and FeCl_3 (8 mmol, 2.1 g) was dissolved in deionized (DI) water (100 mL). At that time, the resultant mixture was stirred mechanically under the argon atmosphere at 80 °C for 10 min. After that, 4 grams of hydrotalcite (I) and NaOH (100 mL, 5%) were added to the solution simultaneously. The resultant brown mixture was stirred for 24 hours at 80 °C. Eventually, the mixture was allowed to cool to room temperature, and then Fe_3O_4 /HT was separated magnetically using an external

magnetic field, washed several times with deionized (DI) water to reach pH=7. Consequently, Fe₃O₄@HT (II) was dried overnight in a vacuum oven at 50 °C.

2.4. Fe₃O₄/HT-SH (III) synthesis

In the following, 1 gram of Fe₃O₄/HT was dispersed ultrasonically in 50 mL of dry toluene for 30 min. Then 3.5 mL (18.5 mmol) of (3-Mercaptopropyl)trimethoxysilane (MPTMS) was added dropwise to the corresponding mixture and was refluxed for 48 hours. Afterward, the resultant Fe₃O₄/HT-SH (III) was then separated using an external applied magnetic field and washing with dry toluene (each 3 × 10 mL) and dried for 16 hours at 25 °C.

2.5. Fe₃O₄/HT-SH-Ag nanoparticles (IV) synthesis

1.0 gram of Fe₃O₄/HT-SH-Ag was dispersed ultrasonically in 20 mL of deionized (DI) water for 30 min at room temperature. Then 3.4 grams (20 mmol) of AgNO₃ in 20 mL of deionized (DI) water was added to the mixture underwent stirred vigorously at 60 °C. Later, the solution of 0.02 g (20 mmol) of sodium borohydride in 20 mL of deionized (DI) water was added to the corresponding reaction under stirred at 60 °C for 10 h. Finally, Fe₃O₄/HT-SH-Ag (IV) was separated by an external magnetic field, washed via deionized water (each 2 × 50 mL), and then dried into the oven (50 °C) for 12 hours.

2.6. General procedure for the oxidation of benzyl alcohols:

Fe₃O₄/HT-SH-Ag (0.007 g, 4.0 mol%) was added to mixture of benzyl alcohol and TBHP (0.5 mmol) in EtOH (0.5 mL) at 65 °C. The reaction process was monitored via TLC. In the end, the Fe₃O₄/HT-SH-Ag was removed using an external magnetic field after reaction completion, washed via EtOH, dried, and reused for several consecutive runs. The resultant product was purified using plate chromatography by EtOAc/*n*-hexane (3:10) solvent mixture.

Selected spectral data:

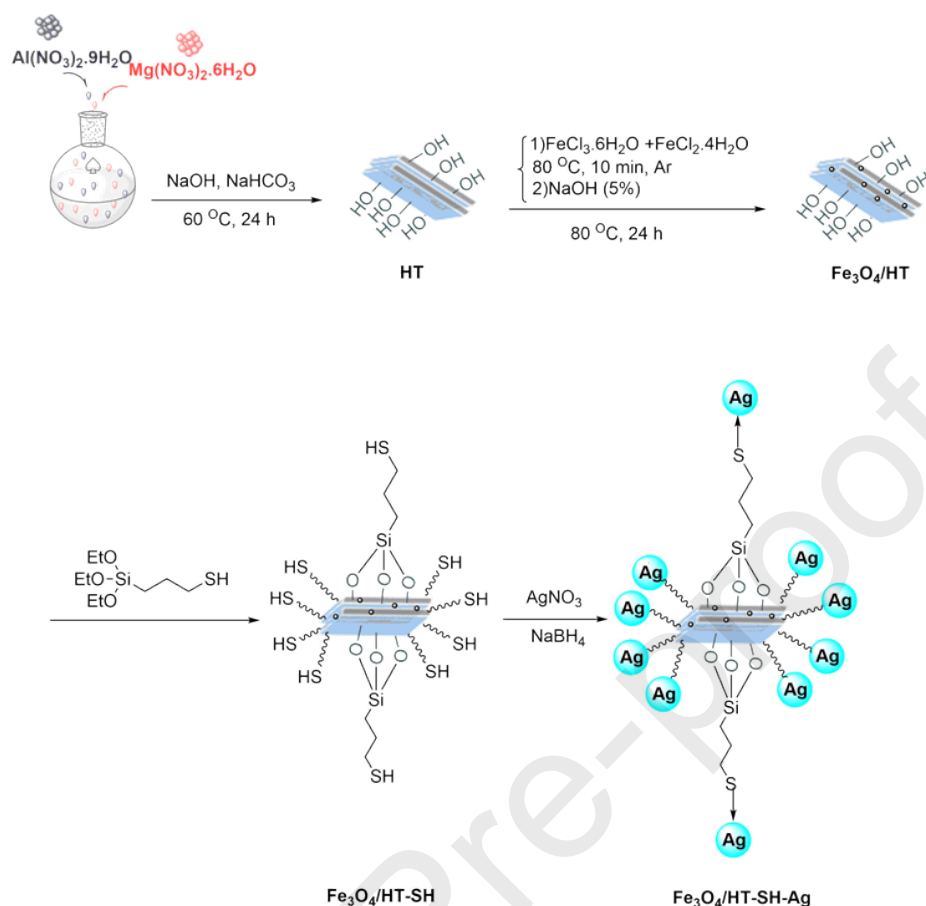
2-chlorobenzaldehyde (Compound 2, Table 3): $^1\text{H-NMR}$ (CDCl_3 , 300 MHz) δ (ppm): 7.295-7.959 (m, 4H, Ph), 10.507 (s, 1H). $^{13}\text{C-NMR}$ (CDCl_3 , 300 MHz) δ (ppm): 189.818 (C=O), 137.957 (C), 135.145 (CH), 132.476 (C), 130.625 (CH), 129.389 (CH), 127.313 (CH).

4-hydroxybenzaldehyde (Compound 4, Table 3): $^1\text{H-NMR}$ (CDCl_3 , 300 MHz) δ (ppm): 6.944-6.972 (2H, Ph), 7.749-7.778 (2H, Ph), 9.789 (1H), 10.616 (1H, OH). $^{13}\text{C-NMR}$ (CDCl_3 , 300 MHz) δ (ppm): 191.247 (C=O), 163.814 (C), 132.534 (CH), 128.897 (C), 116.309 (CH).

4-methylbenzaldehyde (Compound 6, Table 3): $^1\text{H-NMR}$ (CDCl_3 , 300 MHz) δ (ppm): 2.435 (s, 3H, CH_3), 7.318-7.344 (d, 2H, Ph), 7.768-7.795 (d, 2H, Ph), 9.962 (s, 1H). $^{13}\text{C-NMR}$ (CDCl_3 , 300 MHz) δ (ppm): 192.001 (C=O), 145.557 (C), 134.206 (CH), 129.844 (CH), 129.722 (CH), 21.855 (CH_3).

3. Results and discussion:

HT was effortlessly prepared with the co-precipitation procedure. For the preparation of $\text{Fe}_3\text{O}_4/\text{HT}$ (II), HT (I) was used through an alkaline mixed salt-solution of Fe^{2+} and Fe^{3+} . Subsequently, the surface of $\text{Fe}_3\text{O}_4/\text{HT}$ has been modified with (3-Mercaptopropyl) trimethoxysilane (MPTMS) to obtain $\text{Fe}_3\text{O}_4/\text{HT-SH}$ (III). Finally, $\text{Fe}_3\text{O}_4/\text{HT-SH-Ag}$ (IV) was prepared by the immobilization of Ag onto $\text{Fe}_3\text{O}_4/\text{HT-SH}$ (III) in EtOH (Scheme 2).



Scheme 2. Preparation of catalyst ($\text{Fe}_3\text{O}_4/\text{HT-SH-Ag}$)

The catalyst was characterized by utilizing a variety of instrumental analyses like X-ray powder diffraction (XRD), field emission scanning electron microscopy (FE-SEM), Fourier transform infrared spectroscopy (FT-IR), transmission electron microscopy (TEM), vibrating sample magnetometer (VSM), thermogravimetric analysis (TGA), inductively coupled optical emission spectroscopy (ICP-OES), energy-dispersive X-ray (EDX), and CHNS analysis.

The FTIR spectra of HT (I), $\text{Fe}_3\text{O}_4/\text{HT}$ (II), $\text{Fe}_3\text{O}_4/\text{HT-SH}$ (III), and $\text{Fe}_3\text{O}_4/\text{HT-SH-Ag}$ (IV) are represented in Figure 1(a-d). The existence of a strong-broad peak at 3473 cm^{-1} indicates symmetric OH stretching vibration of Al-OH and Mg-OH onto the hydrotalcite surface (Figure 1a). Besides, vibration absorption at 1637 cm^{-1} shows the stretching vibrations associated with the water molecules in the hydrotalcite structure. Meantime, the presence of peaks at 1372 , 671 cm^{-1} indicates the C-O asymmetric stretching vibration mode (representative the attendance of

CO_3^{2-}) and the bending frequency of CO_3^{2-} , respectively. This demonstrates that the CO_3^{2-} is existing between hydroxalcalite layers [7]. At 1366 cm^{-1} , peak intensity decreased in the $\text{Fe}_3\text{O}_4/\text{HT}$ (II) compared with HT, indicating that the HT (I) was magnetized by the Fe_3O_4 [20]. Likewise, the broad absorption of approximately $565\text{--}789\text{ cm}^{-1}$ shows the stretching vibration associated with Fe-O, which was covered with Mg-O and Al-O bonds (Figure 1b). Figure 1c, shows two new absorption bands have confirmed the FT-IR of $\text{Fe}_3\text{O}_4/\text{HT}-(\text{CH}_2)_3\text{SH}$ (III), functionalization with (3-mercaptopropyl)trimethoxysilane (MPTMS) onto the surface of $\text{Fe}_3\text{O}_4/\text{HT}$ (II) at 2851 , and 2931 cm^{-1} (relating to the stretching vibration of $\text{C-H}_{(\text{sp}^3)}$). As shown in Figure 1c, the presence of peak around $1000\text{--}1250\text{ cm}^{-1}$ indicates Si-O-H and Si-O-Si bonds, and as well as $-\text{SH}$ vibration is as well as seen in the 2500 cm^{-1} region as a weak peak.

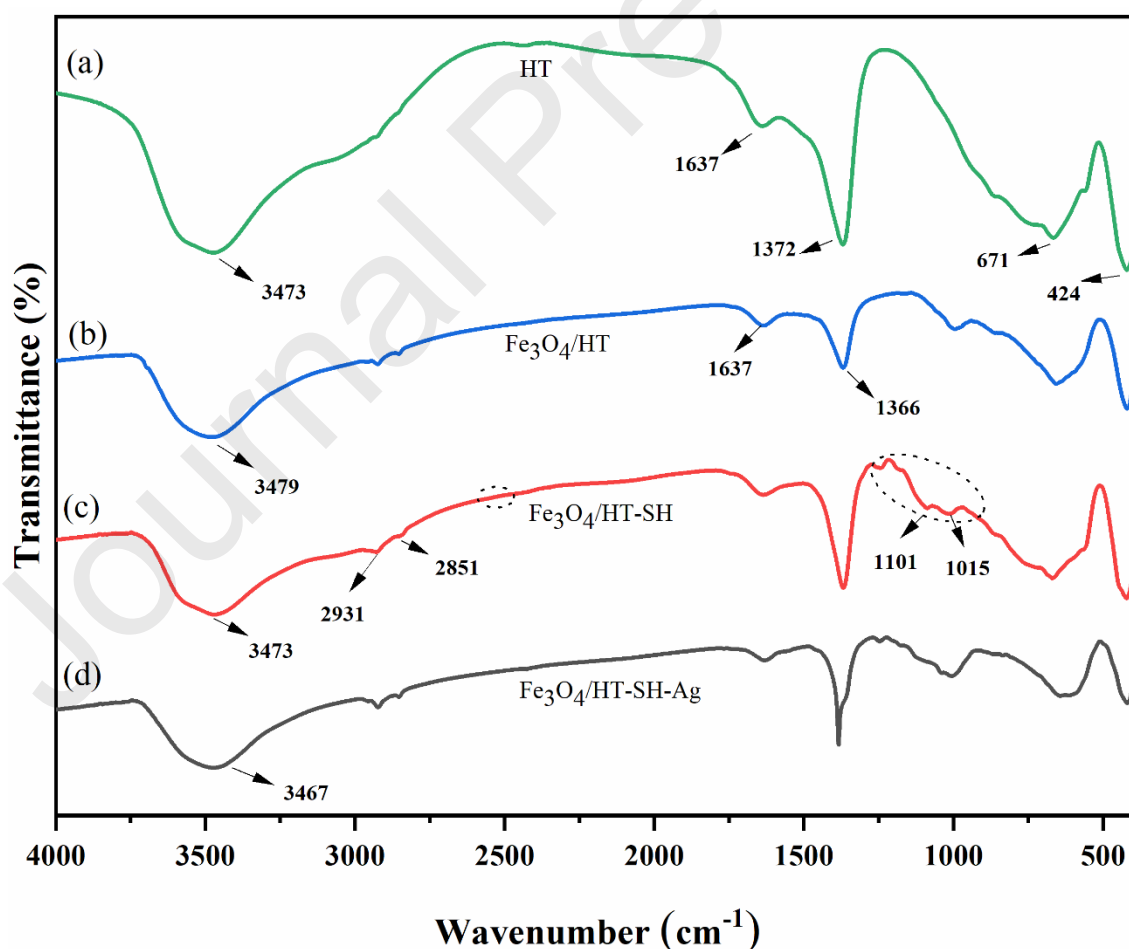


Figure 1. FT-IR spectra of HT (a), $\text{Fe}_3\text{O}_4/\text{HT}$ (b) and $\text{Fe}_3\text{O}_4/\text{HT-SH}$ (c) $\text{Fe}_3\text{O}_4/\text{HT-SH-Ag}$ (d),

The crystal structure of catalysts was examined by X-ray diffraction analysis. The XRD patterns of HT (I), Fe₃O₄/HT (II), and Fe₃O₄/HT-SH-Ag (IV) have been shown in Figure 2 (a-c). The peaks appearing in the diffraction pattern of hydrotalcite (HT) nanoparticles at $2\theta = 11.21^\circ, 22.61^\circ, 34.51^\circ, 38.01^\circ, 45.71^\circ, 60.31^\circ,$ and 61.51° , respectively, belong to plates (003), (006), (012), (015), (018), (110), and (113) respectively [21]. The attendance of new peaks at $2\theta = 30.36^\circ, 35.76^\circ, 43.47^\circ, 57.51^\circ,$ and 63.11° matched well with indices (220), (311), (400), (511), and (440), that were fully consistent with the existence of the magnetic Fe₃O₄ in the HT (I) structure [20]. The four peaks appearing in $2\theta = 38.116^\circ, 44.3^\circ, 64.445^\circ,$ and 77.339° were corresponding to (111), (200), (220), and (311) indices. The pattern was fully in agreement with the Ag nanoparticle in the HT structure (refer. Code: 03-065-2871) [22–24]. The average size of the catalyst was calculated using the Debye-Scherrer's equations:

$$d = 0.9 \lambda / \beta \cos \theta$$

Where λ is the source wavelength (for Cu K $\alpha = 0.154$ nm), β is the width of the XRD peak at half maximum height, and θ is the Bergg diffraction angle. Therefore, the particle size of Fe₃O₄/HT-SH-Ag was calculated as 27 nm.

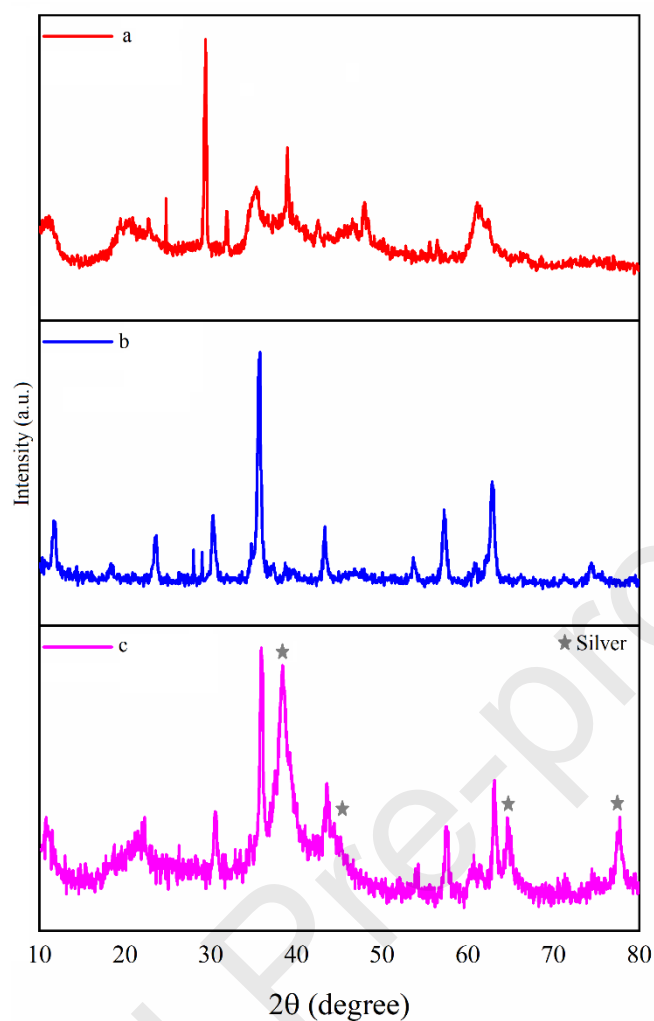


Figure 2. The XRD patterns of (a) HT (I), (b) $\text{Fe}_3\text{O}_4/\text{HT}$ (II) and (c) $\text{Fe}_3\text{O}_4/\text{HT-SH-Ag}$

The morphology of $\text{Fe}_3\text{O}_4/\text{HT-SH-Ag}$ (IV) was studied by the FE-SEM method (Figure 3). According to Figure 3, the as-synthesis HT (I) reveals irregular plate-like morphology, demonstrating the properties of layered materials.

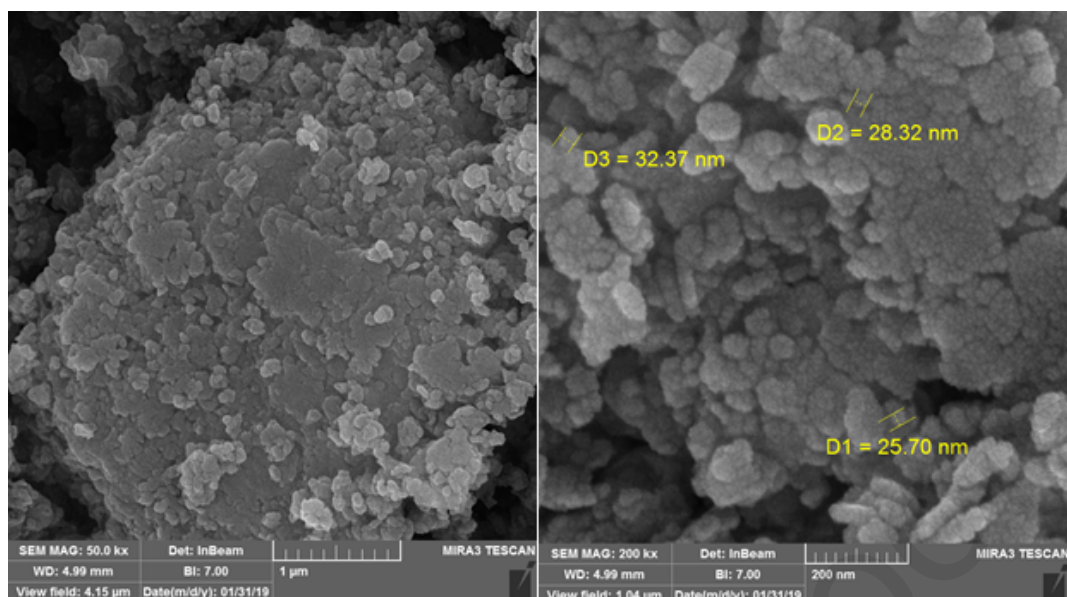


Figure 3. SEM images of $\text{Fe}_3\text{O}_4/\text{HT-SH-Ag(IV)}$

Moreover, the EDS analysis proved Mg, Al, C, O, S, Fe, and Ag elements in the catalyst structure (Figure 4). Also, great intensity Ag showed doping successfully and coordination of Ag onto $\text{Fe}_3\text{O}_4/\text{HT-SH}$ (III). The important point is no impurity elements were observed in the catalyst structure.

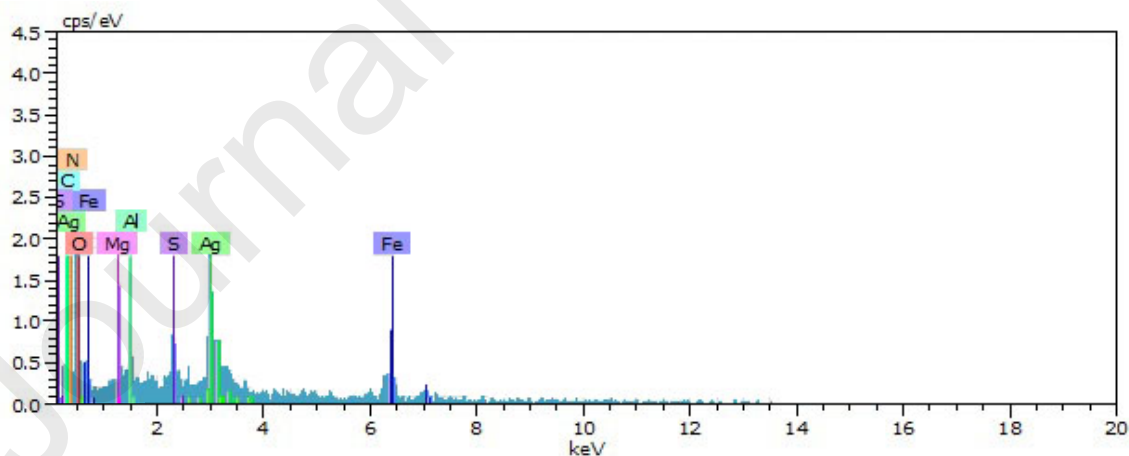


Figure 4. The EDS analysis of $\text{Fe}_3\text{O}_4/\text{HT-SH-Ag(IV)}$

Likewise, TEM analysis was performed to get information about the morphology and structure of $\text{Fe}_3\text{O}_4/\text{HT-SH-Ag(IV)}$. As revealed in Figure 1S, HT (I) is plate-like in shape with the nonuniformly entrapped Fe_3O_4 nanoparticles in its matrix. Moreover, a distribution histogram

of Fe₃O₄/HT-SH-Ag (IV) showed that the average diameter of the catalyst is 13-25 nm (see supporting information, Figure 2S).

Figure 3S illustrates the study of the magnetic behavior of Fe₃O₄/HT (II) and Fe₃O₄/HT-SH-Ag (IV) using VSM analysis. The saturation magnetization of Fe₃O₄/HT (II) and Fe₃O₄/HT-SH-Ag (IV) catalysts are 18.837 and 12.715 emu.g⁻¹, respectively (see supporting information, Figure 3Sa,b). The magnetization decrease of 6.122 emu.g⁻¹ shows the successful functionalization of Fe₃O₄/HT with (3-mercaptopropyl) trimethoxysilane (MPTMS) and Ag (see supporting information, Figure 3Sa,b). Despite this significant reduction, the nanoparticles were effortlessly separated from the reaction environment with a simple external magnetic field.

Besides, the ICP analysis revealed that 183.43 mg equal 1.7 mmol of Ag was anchored on 1 gram of the catalyst.

Catalytic studies:

The catalytic activity of Fe₃O₄/HT-SH-Ag (IV) was examined in the oxidation of alcohols. All oxidation reactions of data are presented in Table 1. In the early stages of the study, 4-chlorobenzyl alcohol (4-Cl BzOH) was selected as a model substrate to obtain optimum circumstances for the oxidation of alcohol to relevant aldehyde. The reaction was done in the absence of Fe₃O₄/HT-SH-Ag (IV) and the attendance of the *tert*-butyl hydroperoxide (TBHP) in EtOH as a green solvent at 65 °C (Table 1, entry 1). It was turned out that the corresponding product was not produced even after a long time (120 min). The fundamental role of Fe₃O₄/HT-SH-Ag was highlighted in the oxidation of alcohols (ROH), when in a set of tests, the model reaction was carried out in the presence of AgNO₃, HT (I), Fe₃O₄/HT (II) (Table 1, entries 2-4).

According to Table 1, Fe₃O₄/HT-SH-Ag (IV) is the utmost effective catalyst that makes the maximum yield of the relevant product in a shorter time in model reaction. To determine the

optimal circumstances, the effect of temperature, and the catalyst loading on the rate of the reaction and also on the yield of the relevant product was also examined. It could be observed that using 0.044 mol% of $\text{Fe}_3\text{O}_4/\text{HT-SH-Ag}$, a significant yield of the corresponding product was seen at 65 °C (Table 1, entry 5-12).

Additional to increase the product yield, the solvent effect was studied. For this aim, water and also several organic solvents (EtOH, EtOH/ H_2O , EtOAc, and CH_3CN) were investigated. The results showed that EtOH and CH_3CN are the best solvents for the reaction. Newly, the request for green chemical synthesis processes and good efficiency has become more necessary. Since EtOH is a green solvent, it was chosen as the solvent (Table 1, Entry 6, 13-17).

Subsequently, we examined the requirement of the oxidant (TBHP) for the oxidation of alcohols (ROH) with the $\text{Fe}_3\text{O}_4/\text{HT-SH-Ag}$ (IV) catalyst.

Table 1. Optimization of various reaction parameters for alcohol oxidation

Entry	Catalyst (mol%)	Solvent	Temp. (°C)	Time (min)	Yield (%)
1	-	EtOH	70	45-120	-
2 ^a	0.007 (g)	EtOH	70	45-120	20
3 ^b	0.007 (g)	EtOH	70	45-120	40
4 ^c	0.007 (g)	EtOH	70	45-120	50
5	0.044	EtOH	75	45	60
6	0.044	EtOH	65	45	90
7	0.044	EtOH	50	45	25
8	0.044	EtOH	40	45	20
9	0.019	EtOH	65	45	60
10	0.032	EtOH	65	45	80
11	0.063	EtOH	65	45	75
12	0.19	EtOH	65	45	70
13	0.044	H_2O	65	45	40
14	0.044	EtOAc	65	45	85
15	0.044	MeCN	65	45	90
16	0.044	EtOH (1:1) H_2O	65	45	60
17	0.044	Toluene	65	45	10

Reaction conditions: 4-chlorobenzyl alcohol (0.25 mmol), TBHP (0.25 mmol)

^a The reaction was carried out in the presence of AgNO_3 . ^b The reaction was performed in the presence of HT (I). ^c The reaction was done in the presence of $\text{Fe}_3\text{O}_4/\text{HT}$ (II)

Alcohol oxidation without TBHP does not indicate any product formation, which we examined in the use of other oxidants like O₂, H₂O₂, air, and Oxone to the reaction model and seen that these oxidants are not active for alcohol oxidizer and no the product is not produced with good efficiency (Table 2, Entry 1-4).

The amount of oxidant (TBHP) is a significant factor influencing the conversion and selectivity in the corresponding reaction. The influence of the substrate to an oxidizing molar ratio was then investigated, and the outcomes are shown in Table 2, entries 5-8.

Table 2. optimization of various oxidants for alcohol oxidation

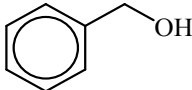
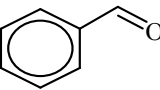
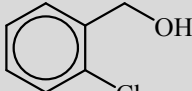
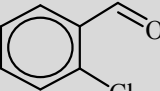
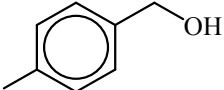
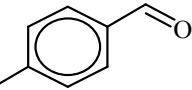
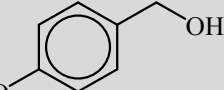
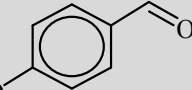
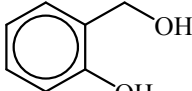
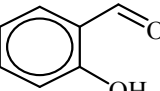
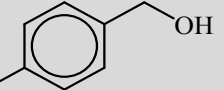
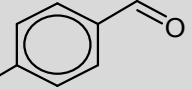
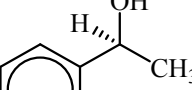
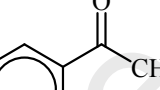
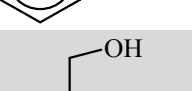
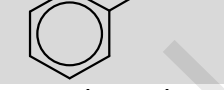
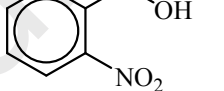
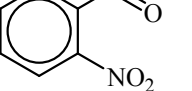
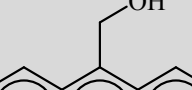
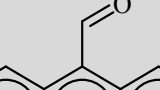
Entry	Oxidant (mmol)	Yield
1	Air	-
2	H ₂ O ₂	30
3	O ₂	-
4	Oxone	15
5	TBHP (0.125)	60
6	TBHP (0.187)	70
7	TBHP (0.25)	90
8	TBHP (0.35)	90

Reaction conditions: 4-chloro benzyl alcohol (0.25 mmol), catalyst (0.044 mol%) in EtOH (0.5 ml)

To discover the amplitude and limitations of the reaction, as well as the efficacy of Fe₃O₄/HT-SH-Ag (IV), many aromatic alcohols have both electron-releasing and electron-withdrawing groups, were selected and carried out under optimal conditions (Table 3).

All of them were reacted effectively and obtained the products with good efficiency. It has been shown that aromatic alcohols counting electron-releasing react faster than electron-withdrawing groups.

Table 3. The oxidation of different alcohols with Fe₃O₄/HT-SH-Ag

Entry	Alcohol	Product	Time (min)	Yield
1			60	82
2			90	75
3			45	90
4			90	60
5			120	60
6			60	90
7			60	82
8			60	95
9			90	80
10			120	65
11			120	50
12			120	42
13			120	40
14			150	60

Reaction conditions: benzyl alcohol (0.25 mmol), TBHP (0.25 mmol) catalyst (0.044 mol%), at 65 °C in EtOH as solvent

Catalyst Recycling

Recyclability of Fe₃O₄/HT-SH-Ag was investigated towards oxidative alcohol (ROH) via TBHP to found the general applicability of the catalyst system presented. During each run catalytically, Fe₃O₄/HT-SH-Ag was separated from the reaction medium by using an external magnetic field and washed three times with H₂O and hot ethanol to remove traces of organic compounds are absorbed, followed with a vacuum oven (80 °C) for 6 hours. The dried Fe₃O₄/HT-SH-Ag was utilized for the next catalytic performance. The Fe₃O₄/HT-SH-Ag utilized for six continuous runs with negligible reduction in the efficiency of product demonstrating the Fe₃O₄/HT-SH-Ag reusability, the outcomes are presented in Table 4.

Also, the ICP-OES analysis presented that the freshly synthesized catalyst has 183.43 mg, or 1.70 mmol of Ag per 1 gram of Fe₃O₄/HT-SH-Ag, while the 6th reused catalyst has 174.25 g, or 1.615 mmol of Ag per 1 gram of Fe₃O₄/HT-SH-Ag. It shows that 95% of Ag can be found in the catalyst structure after six runs. As shown in Figure 4S, the FT-IR spectrum of the recovered catalyst is completely similar to that of the freshly prepared catalyst, reflecting approval of the catalyst under reaction circumstances.

Table 4. Recycling of Fe₃O₄/HT-SH-Ag towards oxidation of alcohols

Entry	Run	Time (min)	Yield
1	1	45	90
2	2	45	90
3	3	45	87
4	4	45	85
5	5	45	85
6	6	45	82

Reaction conditions: 4-chlorobenzyl alcohol (0.25 mmol), TBHP (0.25 mmol), Fe₃O₄/HT-SH-Ag (0.044 mmol%), 65 °C, in EtOH as a solvent.

To understand the properties of Fe₃O₄/HT-SH-Ag, we compare the results of the oxidation of benzyl alcohols with other heterogeneous catalysts, as presented in Table 5.

Table 5. Comparison of results by Fe₃O₄/HT-SH-Ag with various catalysts

Entry	Catalyst	Solvent/Oxidant	Time (min)	Yield (%)	Ref.
1 ^a	Fe ₃ O ₄ MNPs	H ₂ O/H ₂ O ₂	30	89	[25]
2 ^a	Fe ₃ O ₄ @C	H ₂ O/H ₂ O ₂	2880	94	[26]
3 ^b	Fe ₃ O ₄ @SiO ₂ /Ru(OH) _x	Toluene/O ₂	300	95	[27]
4 ^a	Fe ₃ O ₄ /HT-SH-Ag	EtOH/TBHP	45	90	This work

Reaction condition: 4-chloro benzyl alcohol ^a, benzyl alcohol ^b

Conclusion:

In brief, we have successfully synthesized Ag immobilized on modified magnetic hydrotalcite (Fe₃O₄/HT-SH-Ag) from easily available materials. The exact characterization of Fe₃O₄/HT-SH-Ag using spectroscopic and microscopic techniques showed that this novel catalyst has a plate-like shape with an average size of 13-25 nm, superparamagnetic behavior, and 1.7 mmol.g⁻¹ Ag loading. We have introduced a simple and efficient procedure for oxidizing alcohols to the relevant carbonyl compounds in the presence of Fe₃O₄/HT-SH-Ag catalyst in ethanol as a solvent with TBHP at 65 °C. The advantages of this procedure are the use of cheap and green materials, simple procedure, quick reaction periods, effortlessness, high efficacy, and moderated reaction circumstances. Effortless separation of the catalyst with the help of an external magnet and reusability of the catalyst to 6 runs without a noteworthy reduction in activity, the hopeful points of the method are presented, which makes it a good and suitable method for the synthesis of aldehydes and ketones. It is important to note that the catalyst is not sensitive to moisture, and air and there is not much sense to use or maintain it.

Acknowledgments

We gratefully acknowledge the support of this work by the University of Birjand.

References:

- [1] H. Mimoun, The role of peroxymetallation in selective oxidative processes, *J. Mol. Catal.* 7 (1980) 1–29. doi:10.1016/0304-5102(80)85001-2.
- [2] S. Bhunia, D. Saha, S. Koner, MCM-41-supported oxo-vanadium(IV) complex: A highly selective heterogeneous catalyst for the bromination of hydroxy aromatic compounds in water, *Langmuir*. 27 (2011) 15322–15329. doi:10.1021/la202094p.
- [3] M.J. Climent, A. Corma, P. De Frutos, S. Iborra, M. Noy, A. Velty, P. Concepción, Chemicals from biomass: Synthesis of glycerol carbonate by transesterification and carbonylation with urea with hydrotalcite catalysts. The role of acid-base pairs, *J. Catal.* 269 (2010) 140–149. doi:10.1016/j.jcat.2009.11.001.
- [4] P. Liu, Y. Guan, R.A.V. Santen, C. Li, E.J.M. Hensen, Aerobic oxidation of alcohols over hydrotalcite-supported gold nanoparticles: The promotional effect of transition metal cations, *Chem. Commun.* 47 (2011) 11540–11542. doi:10.1039/c1cc15148g.
- [5] T. Mitsudome, Y. Mikami, M. Matoba, T. Mizugaki, K. Jitsukawa, K. Kaneda, Design of a silver-cerium dioxide core-shell nanocomposite catalyst for chemoselective reduction reactions, *Angew. Chemie - Int. Ed.* 51 (2012) 136–139. doi:10.1002/anie.201106244.
- [6] W. Fang, J. Chen, Q. Zhang, W. Deng, Y. Wang, Hydrotalcite-supported gold catalyst for the oxidant-free dehydrogenation of benzyl alcohol: Studies on support and gold size effects, *Chem. - A Eur. J.* 17 (2011) 1247–1256. doi:10.1002/chem.201002469.
- [7] C. Yuan, H. Liu, X. Gao, Magnetically recoverable heterogeneous catalyst: Tungstate intercalated Mg-Al-layered double hydroxides-encapsulated Fe₃O₄ nanoparticles for highly efficient selective oxidation of sulfides with H₂O₂, *Catal. Letters*. 144 (2014) 16–21. doi:10.1007/s10562-013-1129-9.
- [8] B. Reidy, A. Haase, A. Luch, K. Dawson, I. Lynch, Mechanisms of Silver Nanoparticle Release, Transformation and Toxicity: A Critical Review of Current Knowledge and Recommendations for Future Studies and Applications, *Materials (Basel)*. 6 (2013)

- 2295–2350. doi:10.3390/ma6062295.
- [9] D.Q. Feng, G. Liu, W. Wang, A novel biosensor for copper(ii) ions based on turn-on resonance light scattering of ssDNA templated silver nanoclusters, *J. Mater. Chem. B.* 3 (2015) 2083–2088. doi:10.1039/c4tb01940g.
- [10] T.R. deBoer, I. Chakraborty, P.K. Mascharak, Design and construction of a silver(I)-loaded cellulose-based wound dressing: trackable and sustained release of silver for controlled therapeutic delivery to wound sites, *J. Mater. Sci. Mater. Med.* 26 (2015) 1–9. doi:10.1007/s10856-015-5577-1.
- [11] Y. Liu, G. Jiang, L. Li, H. Chen, Q. Huang, X. Du, Z. Tong, Electrospun CeO₂/Ag@carbon nanofiber hybrids for selective oxidation of alcohols, *Powder Technol.* 305 (2017) 597–601. doi:10.1016/j.powtec.2016.10.042.
- [12] S.E. Allen, R.R. Walvoord, R. Padilla-Salinas, M.C. Kozlowski, Aerobic copper-catalyzed organic reactions, *Chem. Rev.* 113 (2013) 6234–6458. doi:10.1021/cr300527g.
- [13] K. Hemmat, M.A. Nasser, A. Allahresani, Olefins oxidation with molecular O₂ in the presence of chiral Mn (III) salen complex supported on magnetic CoFe₂O₄@SiO₂@CPTMS, *Appl. Organomet. Chem.* 33 (2019). doi:10.1002/aoc.4937.
- [14] M.A. Nasser, K. Hemmat, A. Allahresani, E. Hamidi-Hajiabadi, CoFe₂O₄@SiO₂@Co (III) salen complex nanoparticle as a green and efficient magnetic nanocatalyst for the oxidation of benzyl alcohols by molecular O₂, *Appl. Organomet. Chem.* 33 (2019) e4809. doi:10.1002/aoc.4809.
- [15] A.K. Vannucci, J.F. Hull, Z. Chen, R.A. Binstead, J.J. Concepcion, T.J. Meyer, Water oxidation intermediates applied to catalysis: Benzyl alcohol oxidation, *J. Am. Chem. Soc.* 134 (2012) 3972–3975. doi:10.1021/ja210718u.
- [16] T. Mallat, A. Baiker, Oxidation of alcohols with molecular oxygen on solid catalysts, *Chem. Rev.* 104 (2004) 3037–3058. doi:10.1021/cr0200116.
- [17] A. Kamimura, Y. Nozaki, S. Ishikawa, R. Inoue, M. Nakayama, K-birnessite MnO₂: A new selective oxidant for benzylic and allylic alcohols, *Tetrahedron Lett.* 52 (2011) 538–

540. doi:10.1016/j.tetlet.2010.11.114.
- [18] R.A. Sheldon, I.W.C.E. Arends, G.J. Ten Brink, A. Dijkstra, Green, catalytic oxidations of alcohols, *Acc. Chem. Res.* 35 (2002) 774–781. doi:10.1021/ar010075n.
- [19] Y. Xie, W. Mo, D. Xu, Z. Shen, N. Sun, B. Hu, X. Hu, Efficient NO equivalent for activation of molecular oxygen and its applications in transition-metal-free catalytic aerobic alcohol oxidation, *J. Org. Chem.* 72 (2007) 4288–4291. doi:10.1021/jo0705824.
- [20] J. Wang, J. You, Z. Li, P. Yang, X. Jing, M. Zhang, Preparation and characterization of new magnetic Co-Al HTLc/Fe₃O₄ solid base, *Nanoscale Res. Lett.* 3 (2008) 338–342. doi:10.1007/s11671-008-9162-0.
- [21] S. Nishimura, A. Takagaki, K. Ebitani, Monodisperse Iron Oxide Nanoparticles Embedded in Mg–Al Hydrotalcite as a Highly Active, Magnetically Separable, and Recyclable Solid Base Catalyst, *Bull. Chem. Soc. Jpn.* 83 (2010) 846–851. doi:10.1246/bcsj.20100059.
- [22] S.B. Maddinedi, B.K. Mandal, N.K. Fazlur-Rahman, High reduction of 4-nitrophenol using reduced graphene oxide/Ag synthesized with tyrosine, *Environ. Chem. Lett.* 15 (2017) 467–474. doi:10.1007/s10311-017-0610-x.
- [23] S.B. Maddinedi, B.K. Mandal, K.K. Anna, Tyrosine assisted size controlled synthesis of silver nanoparticles and their catalytic, in-vitro cytotoxicity evaluation, *Environ. Toxicol. Pharmacol.* 51 (2017) 23–29. doi:10.1016/j.etap.2017.02.020.
- [24] S.B. Maddinedi, B.K. Mandal, G. Pappu, K.K. Anna, A.R. Ghosh, P.S. Reddy, Synthesis of CuO nanosheets and its applications towards catalysis and antimicrobial activity, *J. Indian Chem. Soc.* 92 (2015) 331–336.
- [25] F. Sadri, A. Ramazani, A. Massoudi, M. Khoobi, R. Tarasi, A. Shafiee, V. Azizkhani, L. Dolatyari, S.W. Joo, Green oxidation of alcohols by using hydrogen peroxide in water in the presence of magnetic Fe₃O₄ nanoparticles as recoverable catalyst, *Green Chem. Lett. Rev.* 7 (2014) 257–264. doi:10.1080/17518253.2014.939721.
- [26] X. Yao, C. Bai, J. Chen, Y. Li, Efficient and selective green oxidation of alcohols by MOF-derived magnetic nanoparticles as a recoverable catalyst, *RSC Adv.* 6 (2016)

26921–26928. doi:10.1039/c6ra01617k.

- [27] V. V. Costa, M.J. Jacinto, L.M. Rossi, R. Landers, E. V. Gusevskaya, Aerobic oxidation of monoterpenic alcohols catalyzed by ruthenium hydroxide supported on silica-coated magnetic nanoparticles, *J. Catal.* 282 (2011) 209–214. doi:10.1016/j.jcat.2011.06.014.

Journal Pre-proofs

Highlights

- Oxidation of alcohols with TBHP were carried out under mild conditions.
- The reused several times without significant loss of reactivity.
- $\text{Fe}_3\text{O}_4/\text{HT-SH-Ag}$ presented excellent efficiency for alcohol oxidation.
- Concise reaction time and excellent yields of products.

Graphical Abstract

